

MONITORING OF WATER CHARACTERISTIC USING THE SYNCHRONOUS  
OBSERVATION DATA OF LANDSAT AND NOAA

Hiroaki Ochiai

Oceanography Department, Toba Merchant Marine College  
1-1 Ikegami-cho, Toba-shi, Mie-ken, Japan 517

ABSTRACT

Using the MSS data obtained from Landsat and AVHRR data obtained from NOAA due to the synchronous observation, the monitoring of water characteristic in some coastal areas around Japan is studied and the effectiveness of the combination of visible data of MSS and thermal infrared data of AVHRR for estimation of marine environment is recognized as well. The analysis procedure is consisted by path radiance correction of Landsat-MSS data and the geometric correction and temperature calibration of NOAA-AVHRR data.

From the results of analysis, the negative correlation between turbidity and sea surface temperature was found in several bay and coastal areas, which indicates that the land origin water from the specific land area such as high population area and industrial area is considered as the main source for water pollution in those areas. On the other hand, the clean contrast between cold water originating from land water and warm water originating from oceanic water under the influences of Kuroshio current, the biggest warm current in the world is carried out from the sea surface temperature pattern derived from NOAA-AVHRR data.

INTRODUCTION

Since the high spatial resolution multispectral data of Landsat-MSS has become available in 1972, many reports have been published in the application of MSS data to the monitoring of marine environment in coastal area (Ref. 1,2,3,4) and the author described the effectiveness of Landsat-MSS data as the real time information in broad area in these reports. From the beginning of 1979 when The Earth Observation Center of National Space Development Agency of Japan is started its performance, the study based on the application of MSS data to the monitoring of marine environment in coastal areas around Japan is rapidly increased and the number of report have been published in Japan for a year is inclining to increase year by year as well as in foreign countries.

Due to the limitation of spectral bandwidth, the information obtained from the analysis of MSS data is focused on the detection of turbidity of water in coastal areas at the time of satellite pass. Moreover, the limitation of field of view of Landsat-MSS, the information carried out from the analysis of MSS data is centered on the estimation of water characteristics in narrow coastal areas.

Although the spatial resolution is lower than that of Landsat-MSS, a meteorological satellite NOAA-AVHRR can offer another very useful information, i.e. sea surface temperature (SST) of the wider area (Ref. 5). In addition, NOAA has an advantage in frequency of observation since it can be observe the same area twice a day while in case of Landsat-MSS it is every 18 day which is a great disadvantage for the monitoring of marine environment.

Thus if the information obtained from Landsat-MSS is highly correlated with that of NOAA-AVHRR, the combined use of the data obtained by both sensors will be great help for daily monitoring of marine environment especially in coastal areas.

In this study, the author described the method of processing and some results of combined use of the Landsat-MSS and NOAA-AVHRR data due to the synchronous observation in the following section.

## INFLUENCE OF OCEANIC WATER TO COASTAL AREA

In almost inlet such as Seto Inland Sea, Osaka bay, Ise bay and Tokyo bay located in southern coast of Japan, the water quality has become seriously bad and we experienced so many occurrence of red tide in recent year. As shown in Fig. 1, red tide, named after its apparent reddish color, is caused by unusually abundant generation of plankton which is often caused by nutrification of water in coastal areas and it causes a shortage of oxygen in the water. It often suffocates fish thus resulting in a great damage to fishing industry in case of severe red tide.

So, the monitoring of water quality especially in warm season is considered as very important for fishing industry and marine environmental administration.

Depend on the author's experience, the occurrence of red tide in coastal areas in Japan is concentrated when Kuroshio current is meandered in great scale influenced by cold water mass (upwelling) located in off southern coast of Honshu, main island of Japan. As shown in Fig. 2 and 3, the flow pattern of Kuroshio current is recognized as two. In case of normal condition, the flow direction of Kuroshio current toward NE along the southern coast of Honshu and the oceanic water influenced by Kuroshio current affects the environmental condition in coastal areas. Namely, the branch current of Kuroshio current forms its flow direction toward the mouth of inlet and the oceanic water can be entered to inlet easily.

When the flow pattern of Kuroshio current shows meandered pattern in great scale, the flow direction of Kuroshio current is very complexity and it affects the flow direction of branch current in some coastal areas such as Kii-suido (entrance of Seto Inland Sea) and Irago-suido (entrance of Ise bay). The flow direction of branch current of Kuroshio current in these areas toward west in this case and the oceanic water can not be entered to inlet and it causes the reduce of water quality in inlet.

From this point of view, the estimation of water characteristics due to the synchronous observation data of Landsat and NOAA is recognized as effective.

## ANALYSIS METHOD

The flow diagram of data processing is shown in Fig. 4. The input data of Landsat-MSS were used the geometrically and radiometrically corrected data (Ref.6) by Earth Observation Center of National Space Development Agency of Japan. The input data of NOAA-AVHRR were used the original data of High Resolution Picture Transmission (HRPT) received by Meteorological Satellite Center of Japan Meteorological Agency located in Kiyose northern part of Tokyo.

### Analysis of Landsat-MSS data

The extraction of the information on the quality of sea water from Landsat-MSS data is usually based on the detection of upwelling back-scattered radiance within the water in the spectral band of Band 4 (0.5-0.6  $\mu\text{m}$ ). Because of low energy of back-scattered radiance over the sea, the Band 4 data over the sea are highly influenced by the effect of atmospheric scattering (path radiance).

Therefore, elimination of the atmospheric effect is essential. The preliminary noise reduction is done by a moving average window of  $3 \times 3$  size, which also reduce the scan-line noise, then Onitsuka's empirical equations (Ref.7) are applied to eliminate atmospheric effect as follows,

$$Lc4 = L4 - Lp4, \quad Lp4 = 0.465 Lp7^{0.260}, \quad Lp7 = L7 \quad (1)$$

Where,  $Lc4$  is the corrected radiance value of Band 4,  $Lp4$  and  $Lp7$  are the path radiance values of Band 4 and Band 7, while  $L4$  and  $L7$  are the calibrated radiance values of Band 4 and Band 7 in Landsat-MSS CCT respectively.

The above correction is carried out for each pixel of MSS data over the sea and finally the corrected data are color-sliced into several radiance levels.

Analysis o

Since  
geometric  
processed  
correction

The g  
actual cor  
following

Where

After  
the Landsa  
with sever

The t  
the intern  
of the the  
following

Where

G and

Where,

The t  
observed w  
 $B(\nu, T)$ ,

Where

The f  
surface ter  
isotherms a  
for isother  
as an outpu

### Analysis of NOAA-AVHRR data

Since the obtained raw AVHRR data contain geometric distortion, the geometric correction must be made in order to superpose the AVHRR data on the processed Landsat-MSS images. The correction procedure consists of tangent correction and affine transformation.

The geometric scheme of the tangent correction is shown in Fig. 5, and the actual correction for each pixel digital count of AVHRR data is carried out by following equation(Ref.8),

$$n = \frac{1}{\Delta\theta 1} \arctan \left\{ \frac{R \sin (m r \Delta \theta 1 / R)}{R + r - R \cos (m r \Delta \theta 1 / R)} \right\} \quad (2)$$

Where,

r ; height of satellite (883Km), R ; radius of the earth (6370Km)  
 n ; pixel digital count before correction  
 m ; pixel digital count after correction  
 $\Delta\theta 1$  ; instantaneous field of view of AVHRR (0.9443mrd)

After the tangent correction, the corrected AVHRR images are superposed on the Landsat images using the affine transformation which is decided in reference with several GCP's on the Landsat and NOAA images.

The temperature calibration of thermal infrared data is carried out using the internal calibration data recorded in a raw AVHRR-CCT and the digital count of the thermal infrared band is converted into brightness temperature by following equation(Ref.8),

$$N = GX + O \quad (3)$$

Where,

N ; observed radiance of the object, X ; CCT count of the object  
 G ; gain, O ; offset

G and O are specified as follows,

$$\begin{aligned} G &= (N_{sp} - N_t) / (X_{sp} - X_t) \\ O &= N_{sp} - G X_{sp} \end{aligned} \quad (4)$$

Where,

$N_{sp}$  ; average radiance of space  
 $N_t$  ; average radiance of internal calibration target (ICT)  
 $X_{sp}$  ; average count corresponding to space radiance  
 $X_t$  ; average count of ICT

The temperature T (°K) and the radiance  $N_t$  of the black body at T (°K) observed with AVHRR are related by the following equation{Planck's formula  $B(\nu, T)$ },

$$N_t = \int_{\nu 1}^{\nu 2} \beta(\nu, T) \hat{\phi}(\nu) d\nu \quad (5)$$

Where,

$\nu$  ; wave number of infrared light  
 $\hat{\phi}(\nu)$  ; response function of the sensor (Ref.9)  
 $\nu 1, \nu 2$  ; lower and upper bound wave number of filter

The final step of the analysis of NOAA-AVHRR data is the generation of sea surface temperature map (SST) from the calibrated thermal infrared image. The isotherms are generated automatically by the computer software. The interval for isotherms is 0.5-1.0 degree in centigrade and the final SST map is obtained as an output from X-Y plotter.

## RESULT OF ANALYSIS

Using the synchronous observation data of Landsat-MSS and NOAA-AVHRR shown in Table 1, the author tried digital analysis due to the processing method described in ANALYSIS METHOD section and satisfactory result are carried out.

The data of NOAA-AVHRR is the same as that of Landsat-MSS except the data set of No. 4 and 5. The observation time of NOAA-6 is between 7:30 and 8:30 a.m., which is about 2 hours earlier than that of Landsat. So, the time difference of both satellite is considered as the boundary of simultaneous observation in the study of marine science.

Fig. 6, 7 and 8 show the superimposed images of the processed Landsat-MSS Band 4 images and the sea surface temperature maps (SST maps) obtained through the analysis of data No. 1, 2 and 3 shown in Table 1. As the temperature values shown in the figures are the values directly obtained from the calibration procedure described in section Analysis of NOAA-AVHRR data and the absolute values are considered to be several degrees in centigrade lower than those of actual SST due to the effect of atmospheric absorption.

In the three figures, the radiance pattern of MSS Band 4 has high correlation with the SST pattern. In Figure 6, for example, in the northern coastal region of Hiuchi-nada and Harima-nada in Seto Inland Sea it can be seen that radiance of MSS Band-4 is higher while SST is lower compared with those of the central and southern parts. On the other hand, the central and southern part of Harima-nada and Kii-suido show relatively low radiance and high SST and this negative correlation suggests that the SST of high turbidity water is lower than that of clean water.

In Fig. 7 and 8, this negative correlation between radiance and SST is also recognized in the western coastal area of Ise-bay and in the north-western part of Kii-suido. In Fig. 7, several interesting circulation patterns are seen in MSS Band 4 within Osaka-bay, however, no remarkable difference in SST in the area of the circulation patterns, which is considered due to the limitation of spatial resolution of NOAA-AVHRR.

## DISCUSSION

The negative correlation between radiance or reflectance of turbid water and its surface temperature found out in the analysis is an interesting fact since the surface temperature of polluted water generally has been considered to be higher than that of clean water. Considering the seasonal effect, the temperature of land originating water is generally lower than that of the water which is a part of warm current (Kuroshio current). Therefore, in Hiuchi-nada and Harima-nada in Fig. 6, the water pollution is considered to be mainly due to the drainage or river effluent originating from the coastal land areas of Chugoku-district and Kinki-district where high population area and industrial area are concentrated respectively.

In the case of Ise-bay (Fig. 8), the polluted and low temperature water is found in northern and western coastal areas, where in addition to large Kiso-river and Ibi-river, the small rivers flow out into the inlet. In Ise-bay, a counterclockwise circulation generally prevails with the result that the western coastal area is highly influenced by the river effluent. Fig. 8 verifies the above stated result. The synchronization of Landsat and NOAA is one of the problems in the analysis. In case of the examples indicated here, time difference of observation by Landsat and NOAA-6 is only 2 hours, therefore synchronization seems to be satisfactory for marine applications. Unfortunately, however, NOAA-6 has become out of order and now only NOAA-7 is available.

The pass of NOAA-7 is 5 or 6 hours later than that of Landsat. Thus, in the coastal region where the influence of tidal current is high and time difference may bring some problems to be the results of analysis. However, in open sea areas, since the SST pattern is considered to be nearly constant during 1 or 2 days and the combination of Landsat and NOAA-7 is considered as effective for investigating both the environmental condition of coastal areas and open sea areas affecting the former condition.

## CONCLUSI

The f  
AVHRR data  
problems of  
remain, th  
routinized  
environmen  
thanks to  
Suzuki, FI  
Kiyoshi Ts  
analysis a  
Research f

## REFERENCES

- 1) Ochiai  
and Lan  
Data, 1
- 2) Ochiai  
mental  
on Remo
- 3) Ochiai  
Sea Sur
- 4) Ochiai  
and NOAA  
1982 (un
- 5) Fisher  
1979, 1
- 6) Tsuchiy  
Society,
- 7) Onitsuka  
Correct  
of Envir
- 8) Tanaka  
Surface  
Geograph  
Vol. 1,
- 9) Lauristo  
NOAA Rad

## CONCLUSION AND ACKNOWLEDGEMENTS

The foregoing analysis indicates that combined use of Landsat-MSS and NOAA-AVHRR data is effective in daily monitoring of wide coastal areas. Although the problems on the synchronization of both data and the spatial resolution of AVHRR remain, the analysis described in this paper is considered a practical and routinized method for utilizing present satellite remote sensing data for marine environmental monitoring. Lastly, the author would like to express his hearty thanks to NASDA for data collection, Dr. Shoji Takeuchi, RESTEC and Mr. Yasushi Suzuki, FIP for data processing. The author is also indebted to Professor Kiyoshi Tsuchiya, Faculty of Engineering, Chiba University for his advice in data analysis and writing the paper. This study is supported by a Fund for Scientific Research from the Ministry of Education.

## REFERENCES

- 1) Ochiai H. and S.Takeuchi; The monitoring of Marine Environmental Problems by Landsat MSS data, The Symposium on Machine Processing of Remotely Sensed Data, 1979.
- 2) Ochiai H. and S.Takeuchi; The Effect of Landsat MSS Data for Marine Environmental Monitoring in Some Coastal Areas of Japan, AGU Fall Meeting, Session on Remote Sensing for Hydrology, 1980.
- 3) Ochiai H. K.Tsuchiya; Application of Remotely Sensed Data to the Detection of Sea Surface Phenomena, Acta Astronautica, 1981,8, 497-509 PP.
- 4) Ochiai H., K.Tsuchiya, S.Takeuchi and Y.Suzuki; Joint Analysis of Landsat-MSS and NOAA-AVHRR Data for Marine Environmental Monitoring, Proceeding of ISTS, 1982 (under printing).
- 5) Fisheries Information Service Center; (a) Report on Use of Satellite Data, 1979, 135 PP. (b) Satellite Information Application, 1982 123 PP (in Japanese)
- 6) Tsuchiya K. and K.Arai; Landsat Ground Station (on data processing), J. of TV Society, 1980, 34, 782-790 PP.(in Japanese)
- 7) Onitsuka M., K.Ohra, N.Okami and J.R.Miller; An Approach to Path Radiance Correction in MSS Images, Fifteenth International Symposium on Remote Sensing of Environment, 1981.
- 8) Tanaka S., T/Sugimura, H.Kimura, H.Nakayama and Y.Ninomiya; Seasonal Earth Surface Temperature Maps of Kansai and Chubu District by NOAA-6 and its Geographical Characteristics, J. of Remote Sensing Society of Japan, 1981, Vol. 1, No. 1.
- 9) Lauriston L., G.J.Nelson, F.W.Port; Data Extraction and Calibration of TIROS/NOAA Radiometers, NOAA Technical Memorandum, 1979, NESS-107.

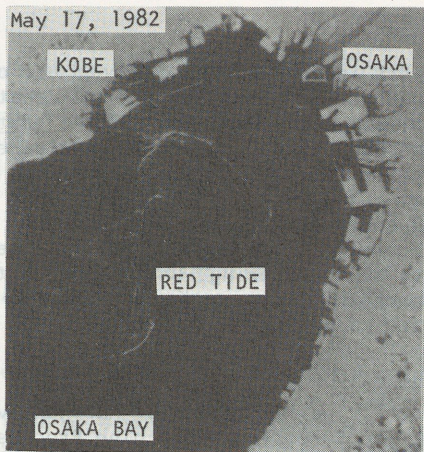


Fig. 1 Red tide pattern indicated in Osaka Bay by Landsat-MSS.

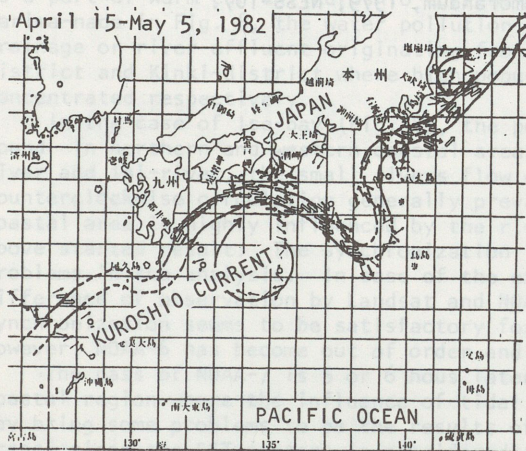
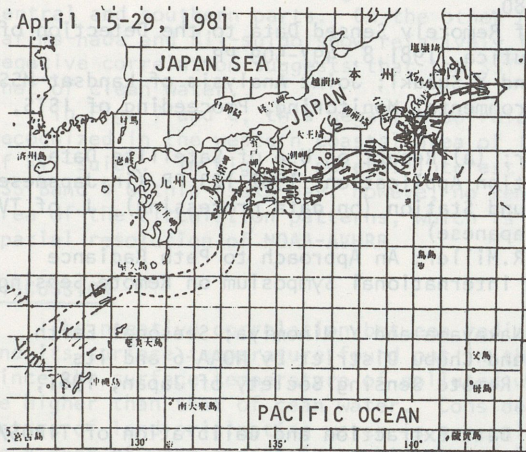


Fig. 2 Flow pattern of Kuroshio Current indicated by ship's observation.

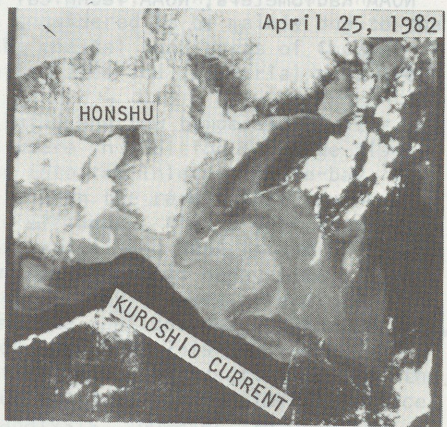


Fig. 3 Flow pattern of Kuroshio Current detected by AVHRR of NOAA-6.

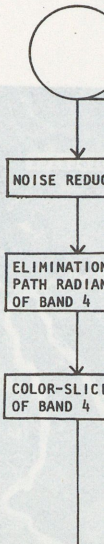


Fig. 1 B... P... A...

NO.	Path
1	119
2	118
3	117
4	115
5	115

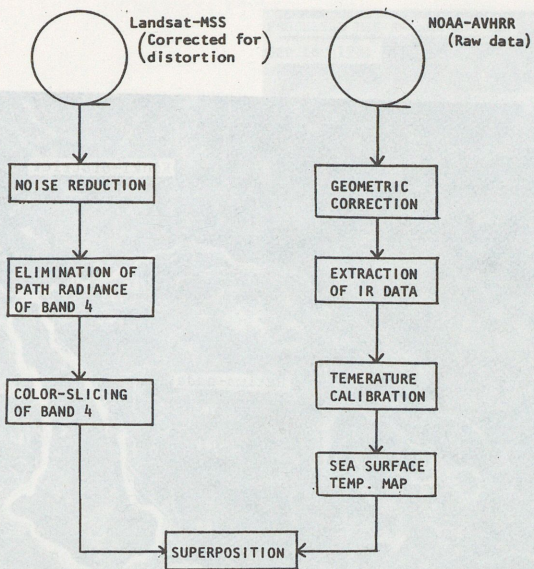


Fig. 1 Block diagram showing superposing process of Landsat-MSS and NOAA-AVHRR data.

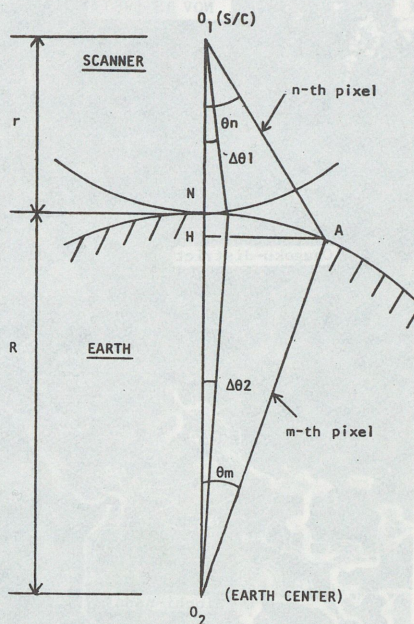


Fig. 2 Geometric scheme of tangent correction.

Table 1 Processed Data List

Landsat			NOAA		Covered sea area
NO.	Path-row	Date	Date	Date	
1	119 - 36	1980.11.15(L-2)	1980.11.15(NOAA-6)		Hiuchi-nada, Harima-nada, and Kii-suïdo
2	118 - 36	1981. 9.16(L-2)	1981. 9.16(NOAA-6)		Osaka-bay and Kii-suïdo
3	117 - 36	1979.11. 1(L-2)	1979.11. 1(NOAA-6)		Ise-bay and Kumano-nada
4	115 - 35	1981. 4.22(L-2)	1981. 4.23(NOAA-6)		Tokyo-bay and Kashima-nada
5	115 - 35	1982. 4.26(L-3)	1982. 4.25(NOAA-6)		Tokyo-bay and Kashima-nada

Fig. 3 Superposed image of Ise-bay and neighboring open sea. (Nov. 1, 1979, No. 3 in Table 1)

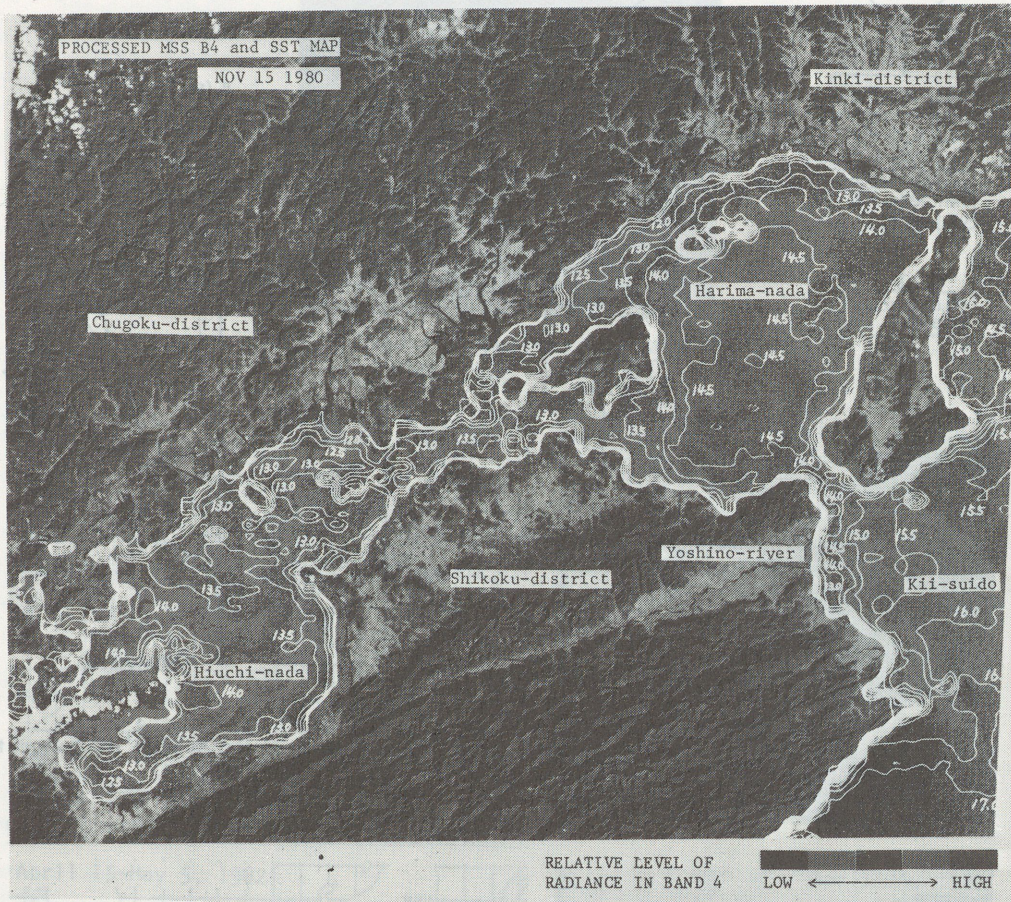
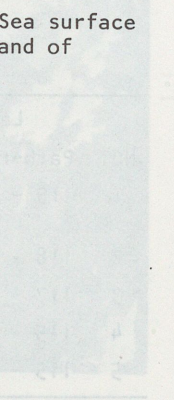
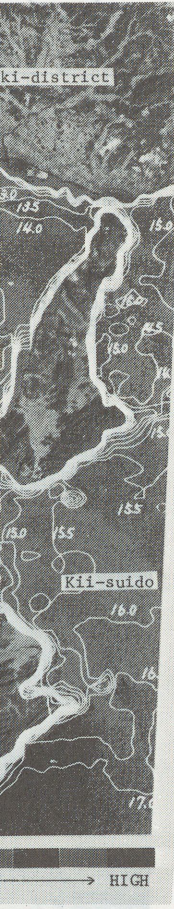


Fig. 6 Superposed image of processed Landsat-MSS band 4 and Sea surface temperature (SST) map derived from thermal infrared band of NOAA-AVHRR data. (Nov. 15, 1980, No. 1 in Table 1)





Sea surface and of

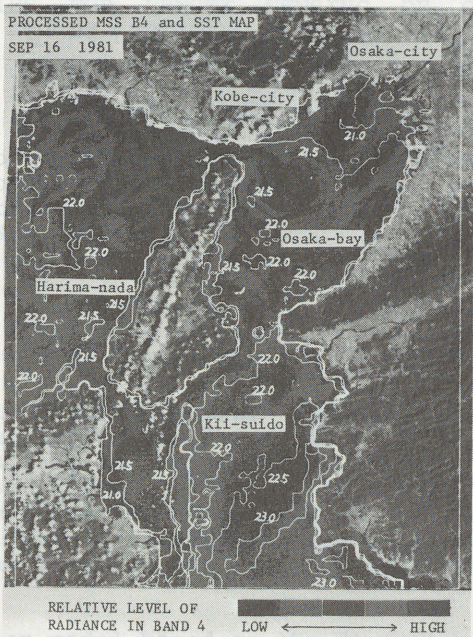


Fig. 7 Superposed image showing the area east Fig. 6. (Sept. 16, 1981, No. 2 in Table 1)

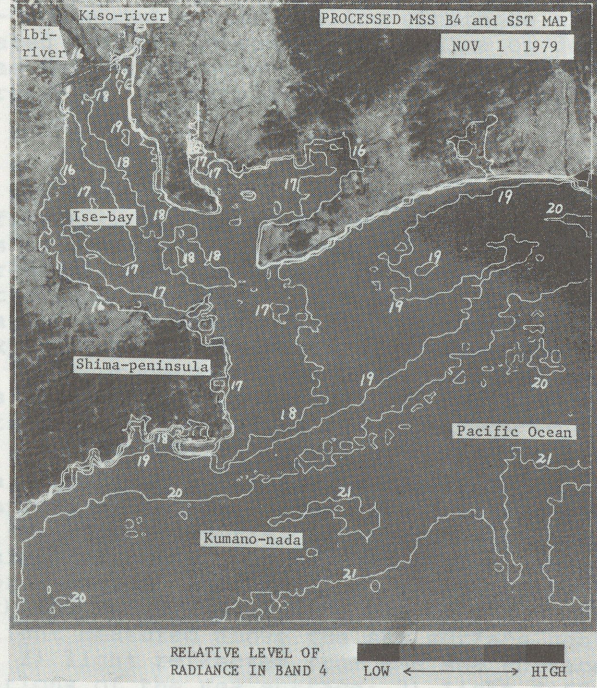


Fig. 8 Superposed image of Ise-bay and neighboring open sea. (Nov. 1, 1979, No. 3 in Table 1)

